

Electrochemical Promotion of Propane and Propene Oxidation on Pt/YSZ

P. Vernoux,^{*,1} F. Gaillard,^{*} L. Bultel,[†] E. Siebert,[†] and M. Primet^{*}

^{*}Laboratoire d'Application de la Chimie à l'Environnement (LACE), UMR 5634 CNRS—Université Claude Bernard Lyon 1, 69622 Villeurbanne Cedex, France; and [†]Laboratoire d'Electrochimie et de Physico-chimie des Matériaux et des Interfaces (LEPMI), UMR 5631 CNRS—INPG—Université Joseph Fourier Grenoble I, BP 75, 38402 Saint Martin d'Hères Cedex, France

Received November 26, 2001; revised February 7, 2002; accepted February 12, 2002

The nonfaradaic electrochemical promotion modification of catalytic activity (NEMCA) was investigated in the total oxidation of propane and propene on Pt films deposited on 8 mol% Y₂O₃-stabilized ZrO₂ solid electrolyte. It was found that propane and propene oxidation exhibit opposite behaviors with respect to the applied overpotentials. Propane oxidation exhibits an electrophobic enhancement (reaction increases upon positive polarization of the catalyst-electrode) while propene oxidation is electrophilic. Upon applied negative overpotential and under an oxygen-rich atmosphere, the rate of propane oxidation strongly decreases, with high values of faradaic efficiency, up to 10,000. Propane and propene oxidation rates were found to be controlled over a wide range of voltage in a reversible way. Catalytic activity measurements under open-circuit voltage conditions, using solid electrolyte potentiometry and temperature-programmed desorption, have been used in order to understand and investigate the origins of this electrochemical promotion. They seem related to different behaviors of propane and propene with respect to their competitive adsorption with oxygen on platinum. Propene adsorbs strongly in competition with oxygen, whereas propane adsorbs weakly. This indicates that the NEMCA behavior of a catalytic reaction is dependent on the oxygen coverage on the catalyst-electrode under open-circuit conditions. © 2002 Elsevier Science (USA)

Key Words: catalytic combustion; propane; propene; platinum; electrochemical promotion; NEMCA.

INTRODUCTION

Catalytic combustion of light hydrocarbons represents one of the nonpolluting and more economical means of heat and energy generation. The use of electrochemistry to activate and control the catalytic process is an expanding domain because of the development of new solid electrolytes. These materials are ionic (cationic or anionic) conductors. In a solid electrolyte cell, using the working electrode as both an electrode and a catalyst, the application of a current or a potential between the catalyst-electrode and an inert counterelectrode can affect the catalytic activity and

the product selectivity, in a reversible and controlled manner. A new concept (1–3), named nonfaradaic electrochemical modification of catalytic activity (NEMCA effect), has also increased the interest in electrochemical promotion because it is not faradaic and thus not limited by the migration rate of ionic species in the solid electrolyte. The NEMCA effect has been observed for a wide range of reactions in the presence of metals such as Pt, Pd, Rh, Au, Ag, and Ni, and of oxides such as IrO₂ and RuO₂. The solid electrolytes used may be O²⁻ conductors like YSZ (Y₂O₃-stabilized ZrO₂) (4–6) or CeO₂ (7), Na⁺ conductors like β''-Al₂O₃ (8, 9) or Na₃Zr₂Si₂PO₁₂ (10), H⁺ conductors like CaZr_{0.9}In_{0.1}O_{3-α} (11, 12) or Nafion (13), F⁻ conductors like CaF₂ (14), and mixed conductors, both ionic and electronic, like TiO₂ (15).

Among the studies on the electrochemical promotion of catalytic activity, much work concerns oxidation of light hydrocarbons on precious metals, such as platinum, deposited on an oxygen ion conductor. The reaction rate under an applied current or potential may reach values up to 100 times higher than what is observed under open-circuit voltage (OCV) conditions. When using YSZ as a solid electrolyte, the increase of the catalytic reaction rate may be up to 1000 times higher than what can be predicted by Faraday's law ($I/2F$, where I is the applied current), considering only O²⁻ ions pumping through the electrolyte toward the catalyst. The former studies on the NEMCA effect, and more particularly the extensive work performed at the Department of Chemical Engineering of the University of Patras (Greece), have led to the definition of some fundamental parameters in order to describe and to quantify the effects of electrochemically promoting a catalytic reaction. The main parameters are as follows:

1. The enhancement factor or faradaic efficiency, Λ , defined by

$$\Lambda = (r - r_o)/(I/nF) = \Delta r/(I/nF), \quad [1]$$

where r_o , in moles of O per second (case of an O²⁻ conductor), is the catalytic rate at OCV, r the catalytic rate under polarization, n the number of exchanged electrons during the electrode reaction ($n = 2$ with an O²⁻ conductor), and

¹ To whom correspondence should be addressed. Fax: +33 4.72.44.81.14. E-mail: Philippe.Vernoux@univ-lyon1.fr.

Δr the catalytic reaction rate change induced by a current I . A catalytic reaction exhibits the NEMCA effect when $|\Lambda| > 1$. A reaction which is accelerated by a negative current or overpotential (oxygen removed from the catalyst surface) exhibits an electrophilic NEMCA behavior and corresponds to a value of Λ lower than -1 . In parallel, when the catalytic reaction is promoted by a positive current or overpotential (oxygen supplied to the catalyst surface), its NEMCA behavior is called electrophobic ($\Lambda > 1$).

2. The rate enhancement ratio, ρ , defined by

$$\rho = r/r_0. \quad [2]$$

In order to investigate the origins of the NEMCA effect, many experiments were carried out using techniques such as X-ray photoelectron spectroscopy (XPS) (16, 17), temperature-programmed desorption (TPD) (18–21), cyclic voltammetry (19, 22), scanning tunneling microscopy (STM) (23), ac impedance spectroscopy (24), Kelvin probe (25, 26), and ultraviolet photoelectron spectroscopy (UPS) (27). It has been established that a change in the electrode overpotential ΔV_{WR} results in a modification of the work function $e\Phi$ of the gas-exposed electrode surface of the porous catalyst film:

$$\Delta(e\Phi) = e\Delta V_{WR}. \quad [3]$$

The theoretical validity of this equation has been discussed in the literature (28–33). The validity of this relationship seems restricted to the cases where outer potential ($\Delta\psi$) variations can be neglected, and this implicates the following conditions:

- Application of moderate overpotentials.
- Low lateral interactions between surface ions.
- Fast surface diffusion of ionic species.

When using YSZ and applying a positive overpotential or current, the NEMCA effect may be attributed to an electrochemical spillover of oxide ions O^{2-} from the solid electrolyte onto the whole gas-exposed catalyst surface. The positive charge, induced by the positive overpotential, on the electrode is compensated for by a negative oxide ion spillover onto the catalyst. This leads to a negligible $\Delta\psi$. The presence of ionic oxygen species $O^{\delta-}$ onto the catalyst surface increases the work function because the dipole moment of these oxygen species on the catalyst-electrode surface is expected to be higher than that of atomic adsorbed oxygen. Indeed, it has been shown (34) that the work function variation can be related to that of the dipole moment by the Helmholtz equation

$$\Delta(e\Phi) = \frac{eN_m}{\epsilon_0} \sum_j \Delta(P_{O,j} \cdot \theta_j) \quad [4]$$

where N_m is the surface metal atom concentration, $e = 1.6 \times 10^{-19}$ C/atom, $\epsilon_0 = 8.85 \times 10^{-12}$ C²/J · m, and $P_{O,j}$, j

corresponds to the dipole moment of each species j present on the catalyst surface at a coverage θ_j .

Moreover, TPD and XPS measurements have shown that the ionic oxygen species $O^{\delta-}$, resulting from the electrochemical pumping, are strongly adsorbed and mainly lead to a decreasing of the strength of their neighbors' bonds between chemisorbed oxygen and the catalyst. Then, the chemisorbed oxygen atoms coming from the gas phase get more weakly bonded and become much more reactive (19, 20).

Upon application of a negative current or overpotential, the thus-induced negative charge on the electrode is compensated for by the backspillover of the negative oxide ions from the catalyst through the electrolyte. The polarization can modify the dipole moments and the work function and, then, the binding strengths of the adsorbed species.

The electrochemical promotion of CH_4 (4), C_2H_4 (35–37), C_2H_6 (6), and C_3H_6 (5) oxidation has been investigated on the Pt/YSZ system. Alkanes (methane and ethane) are reported to exhibit both electrophilic and electrophobic NEMCA behavior. This means that the catalytic rate increases whatever the sign of applied current or polarization. Application of positive overpotentials leads to an increasing of the work function (Φ). As recently stated by Vayenas *et al.* (38), the consequence is that it strengthens the chemisorptive bond of electron-donor adsorbates and weakens the chemisorptive bond of electron-acceptor adsorbates. The result is, here, a weakening of the Pt–O bonds and a strengthening of the Pt–hydrocarbon bonds, both leading to a lowering of the oxygen coverage on platinum. The opposite effect is obtained upon application of negative overpotentials. The promoting effect, whatever the direction of the current, remains partially unexplained and is also dependent on the oxygen content in the reactive mixture.

The oxidation of propene on Pt/YSZ is reported as purely electrophilic (38); the reaction rate increases with a negative current and does not vary with a positive one (5). This means that an increase of the oxygen coverage increases the rate of propene oxidation. In the case of ethylene, the promoting effect can be either electrophilic or electrophobic, depending on the gas-phase composition and on the $P_{O_2}/P_{C_2H_4}$ ratio. The ethylene oxidation exhibits electrophobic behavior in oxygen-rich conditions and electrophilic behavior in ethylene-rich conditions (39). In a general way, the adsorption competition between hydrocarbon and oxygen, i.e., the oxygen coverage on platinum at OCV, is expected to influence the nature and the intensity of the electrochemical promotion effect.

In order to quantify the role of the oxygen coverage on the catalyst-electrode at OCV, the present study is focused on propane and propene oxidation on Pt/YSZ. We selected these hydrocarbons because, in spite of their similar steric factor, they exhibit quite different behavior depending on their strength of adsorption on platinum. Indeed, several

studies (40–42) have shown that alkenes adsorb strongly and compete with oxygen, whereas alkanes adsorb weakly and therefore without significant adsorption competition with oxygen. Propene adsorbs strongly on platinum because of the interaction of its π -orbitals with Pt d-bands (43). Concerning propane oxidation, the limiting step would be the cleavage of a primary C–H bond (44).

In this work, catalytic activity measurements under OCV conditions, solid electrolyte potentiometry (SEP), and temperature-programmed desorption (TPD), were carried out in order to evaluate the oxygen activity on platinum under C_3H_8/O_2 and C_3H_6/O_2 . Finally, catalytic behaviors, upon applying overpotentials, for propane and propene oxidation were compared.

EXPERIMENTAL

Catalytic Activity Measurements

The electrolyte was an yttria-stabilized zirconia (TOSOH powder, 99.99%; average grain size, 0.3 μm), containing 8 mol% yttria, and sintered at 1350°C for 2 h (densification higher than 98%). YSZ disks were 17 mm in diameter and 1 mm thick. The Pt catalyst, in the form of platinum paste (Engelhard-Clal 6926), was deposited on one side of the YSZ pellet and calcined at 600°C for 5 h. Counter- and reference electrodes, both made from gold paste (Engelhard-Clal no. A1644), were deposited on the other side of the electrolyte disk and annealed at 800°C for 1 h. Gold was selected because of its negligible catalytic activity in propane and propene oxidation, as checked via blank experiments under our experimental conditions.

The catalytic properties were evaluated with a fairly conventional automated test bench. The quartz reactor (see Fig. 1) was operated under continuous flowing conditions at atmospheric pressure. The YSZ pellet was placed on a fritted quartz, 18 mm in diameter, with the catalyst-electrode side facing the fritted quartz. The gas flow passed through the porous disk from below and then licked the catalyst. An inner quartz tube was pressed onto the YSZ pellet in order to insure electric contacts. The Viton gaskets, placed in a polypropylene cap, insured the airtightness between the two quartz tubes. All the current collectors were made of gold. A gold mesh was placed between the quartz porous disk and the working electrode. One gold wire, 2 mm in diameter, was welded onto the gold mesh and two others were attached to the reference and counterelectrodes. A tubular furnace (PEKLY JF 9) heated the reactor. The reaction gases were composed of a hydrocarbon, C_3H_6 (Air Liquide, 7710 \pm 231 ppm C_3H_6 in He) or C_3H_8 (Air Products, 8000 \pm 80 ppm C_3H_8 in He), O_2 (Air Liquide, 99.995% purity), and helium (Air Liquide, 99.995% purity). This last one was used as a carrier gas. The gas compositions were controlled by mass flow meters (Brooks, with an accuracy better than 1%). In the following, the gas composition is expressed in parts per million or percentage and the mixtures

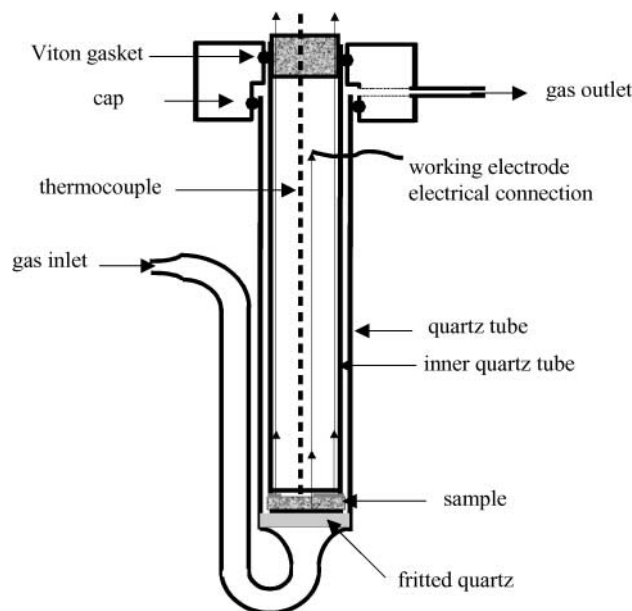


FIG. 1. Schematic drawing of the catalytic reactor.

are described as follows: C_3H_6/O_2 : 2000 ppm/1%. The overall gas flow rate was kept constant at 6.7 ± 0.1 L/h. The product gases were analyzed by two chromatographs. The first one (Intersmat, IGC 120 MB) was equipped with a thermal conductivity detector and a CTR1 column from Alltech (Porapak and molecular sieve), heated at 45°C, which enabled the separation of O_2 , CO_2 , and CO. The second chromatograph (Intersmat, IGC 120 FL) used a Porapak column, heated at 170°C, and analyzed C_3H_6 and C_3H_8 hydrocarbons with a flame ionization detector. A Chromjet analyzer (ThermoQuest) controlled the valve injection system, data acquisition, and integration of chromatographic data. Prior to the catalytic activity measurements, the sample was pretreated in H_2 at 300°C for 1 h in order to reduce platinum. Then, the reactor was purged by helium and allowed to cool to 200°C. Finally, the sample was heated to the working temperature under a flow of helium. Once the reactive mixture flow was admitted into the reactor, the chromatographic analysis was started. The conversion of the hydrocarbons (HC) into CO_2 was defined as

$$HC_{\text{conversion}} = 100 \times P_{CO_2} / (P_{CO_2} + 3 \times P_{HC}), \quad [5]$$

where P_{CO_2} and P_{HC} are the partial pressures of CO_2 and the hydrocarbon (C_3H_8 or C_3H_6) in the outlet gas, respectively. CO_2 is the only carbon-containing oxidation product. Carbon monoxide was not detected, according to our lower detection limit of about 50 ppm. The three electrodes, W (catalyst electrode or working electrode), R (reference), and CE (counterelectrode) were connected to a potentiostat–galvanostat Voltalab 80 (Radiometer Analytical). Voltage or current was applied and measured according to the procedure generally used in conventional three-electrode electrochemical cells.

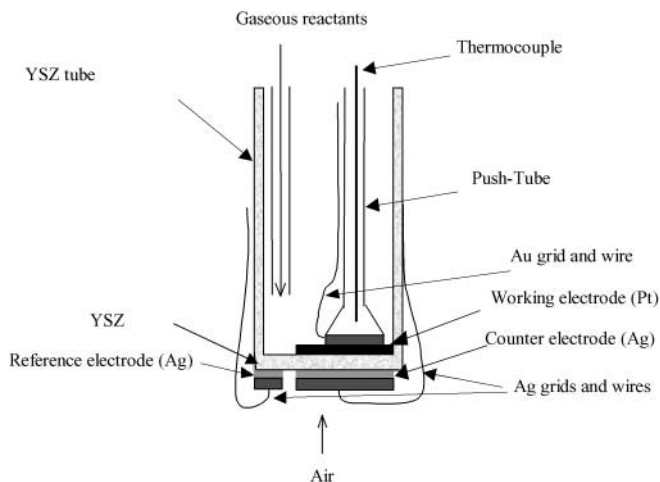


FIG. 2. Schematic drawing of the electrochemical cell used for SEP.

Solid Electrolyte Potentiometry

Solid electrolyte potentiometry (SEP) measurements were carried out in a 2-atm electrochemical cell (Fig. 2). The working electrode together with its current collector was prepared the same as for catalytic tests. The Pt catalyst was calcined at 800°C for 5 h. An inner Pyrex tube was pressed onto the working electrode in order to insure the electric contact. Reference and counterelectrodes were made of Ag paint (DEMETRON 200) and annealed at 650°C for 2 h. The current collectors were Ag meshes attached with Ag wires, 2 mm in diameter. These two electrodes were exposed to air. Torr-Seal[®] adhesive (Varian Vacuum Products) was applied between the top of the YSZ tube and the head of the Pyrex cell, in order to insure the sealing between the two atmospheres. Potential measurements were made using a PGS 201T potentiostat.

Temperature-Programmed Desorption

In order to determine if propane and propene behave differently with respect to adsorption on platinum, a 5 wt% Pt/YSZ powder catalyst was studied by TPD after reaction at low hydrocarbon conversion. The YSZ-supported Pt powder was prepared by impregnation of YSZ with H₂PtCl₆ (Alfa) in aqueous solution. The powder was annealed at 450°C for 1 h in air, in order to decompose the precursor. The specific area of this powdered catalyst was 18 m²/g and the quantity of platinum, determined by chemical analysis, was 4.8 wt%. The catalyst was investigated during hydrocarbon combustion and then by temperature-programmed desorption (TPD). A weight of about 100 mg of the solid was placed on a quartz wool bed in a U-shaped quartz reactor, positioned vertically in a programmable tube furnace. Prior to combustion/TPD experiments, the catalyst was heated at 5°C/min in He flow (1.2 L/h) up to 300°C, then reduced for 1 h in pure H₂ (1.2 L/h). Combustion ex-

periments were performed in a 2000 ppm hydrocarbon/1% O₂/He mixture at a flow rate of 6.7 L/h, established by mass flow controllers, from pure He mixed to 8000 ppm hydrocarbon/He and 5% O₂/He certified mixtures (Air Liquide). A part of the flow of products and reactants exiting the reactor (about 0.6 L/h) was sampled by a heated capillary and analyzed by a VG Gasslab 300 quadrupole mass spectrometer. Signals at $m/e = 16, 18, 28, 32,$ and 44 amu corresponding to O₂⁺, H₂O⁺, N₂⁺ or CO⁺, O₂⁺, and CO₂⁺ ions, respectively, were recorded. Propane concentration in the flow was determined from signals at $m/e = 27, 29,$ and 43 amu, and propene concentration from signals at $m/e = 41$ and 42 amu. The signal at $m/e = 15$ amu was also followed to detect CH₃⁺ species resulting from the hydrocarbon fragmentation. After the catalyst reduction, the reactor was purged by pure He and allowed to cool to 100°C under He flow. Then, the hydrocarbon/O₂/He mixture was admitted into the reactor and the temperature was increased at 5°C/min in order to reach stabilization at about 5% hydrocarbon conversion (temperature was close to 170°C). The combustion was maintained for 30 min and the reactor flushed by He (for 10 min) under isothermal conditions. Then, TPD analysis was performed under He flow (1.75 L/h) at 20°C/min up to 850°C.

RESULTS

Catalytic Activity Measurements under Open Circuit

The catalytic activities of the Pt/YSZ system in the oxidation of C₃H₆ and C₃H₈ are given in Fig. 3. The catalytic activity measurements were performed between 200 and 450°C in 50°C steps, maintained for 30 min. For both C₃H₆ and C₃H₈, the concentrations in hydrocarbon and oxygen are very close and correspond to oxygen-rich mixtures. As expected, catalytic behaviors are different according to the nature of the hydrocarbon. The oxidation of propene is almost complete at 295°C, whereas conversion of propane

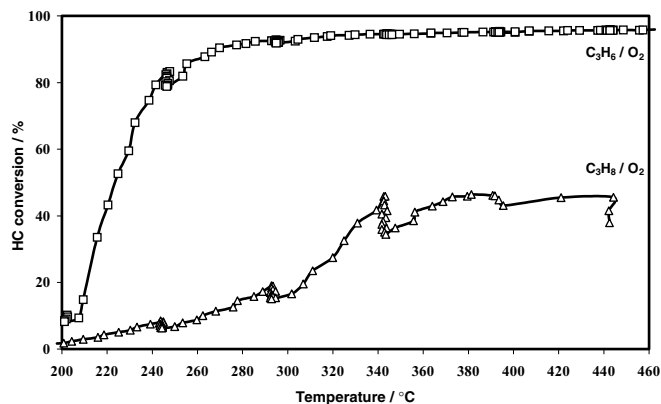


FIG. 3. Hydrocarbon conversion versus temperature at OCV under C₃H₆/O₂: 6860 ppm/8.9% (□) and under C₃H₈/O₂: 7260 ppm/8.86% (△).

does not exceed 45%, even at 450°C. This unusual catalytic behavior could be explained by the particular geometry of the cell. Diffusion limitations could occur at temperatures higher than 350°C and are probably responsible for the non-complete conversion of propane at 450°C, since propane is more difficult to oxidize than propene. Catalytic oxidation of propane shows deactivation during the temperature plateaux, in particular at 350°C (Fig. 3). The origin of the deactivation is not clear. Taking into account the large amount of oxygen in the reactive mixture, this deactivation cannot be explained by carbon deposition on platinum surface. This could be due to the specific microstructure of the Pt electrode-catalyst by comparison with a powdered catalyst.

The beginning temperature of reaction (called lights off in the rest of this paper) is lower by about 50°C in the case of propene. Moreover, the catalytic activity in the propane oxidation gradually increases whereas that of the propene oxidation abruptly increases. Figures 4a and 4b show the variations of propane and propene conversions, respectively, according to oxygen partial pressure at 400°C. With propane, the catalytic activity exhibits a maximum at a

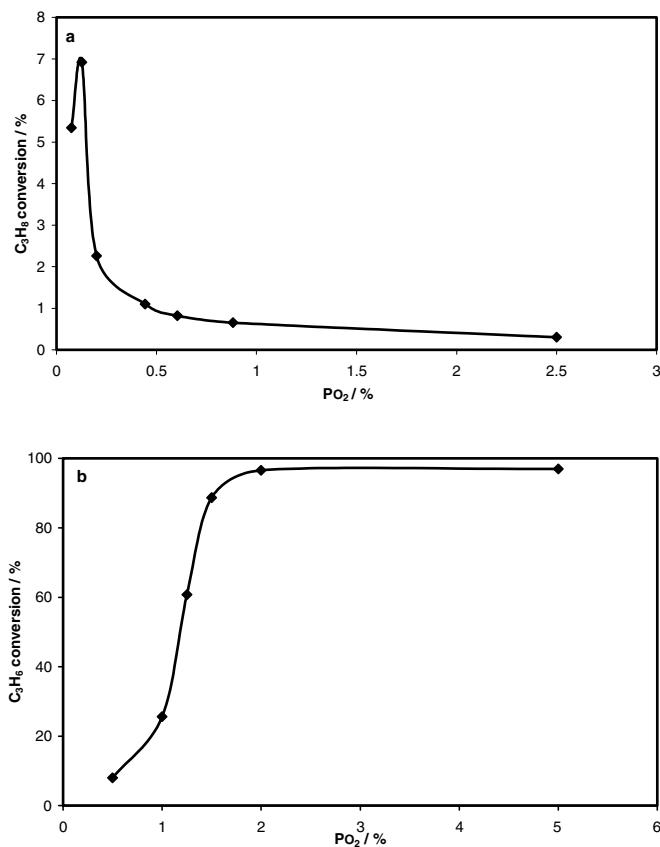


FIG. 4. Propane (a) and propene (b) conversion versus partial pressure of oxygen at OCV. $T = 400^\circ\text{C}$; hydrocarbon concentration = 2000 ppm.

$P_{C_3H_8}/P_{O_2}$ ratio close to one, and decreases when the partial pressure of oxygen increases. On the other hand, with propene, the catalytic conversion highly increases with an increase in the partial pressure of oxygen and stabilizes under oxygen-rich conditions, at P_{O_2} of ca. 2%. Let us recall that the full conversion of 2000 ppm propene requires 0.9 vol% O_2 . In both cases, the carbon mass balance is close to 5%.

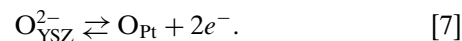
These experiments suggest a competitive adsorption between hydrocarbon and oxygen on platinum surface. For the C_3H_8/O_2 atmosphere, oxygen seems to be more strongly adsorbed than propane on the catalyst surface, which leads to the presence of a conversion maximum when P_{O_2} is varied. Such a maximum corresponds to an oxygen content much lower than that corresponding to the stoichiometry. The same result is reported by Kaloyannis and Vayenas (6) for the oxidation of ethane on Pt/YSZ. In contrast, under C_3H_6/O_2 , the strength of the bond between propene and platinum is stronger than that between oxygen and platinum. This catalytic behavior of the Pt/YSZ system under C_3H_6/O_2 is in good agreement with that reported in the literature (5). These observations could mean that under open-circuit conditions and at low conversion of the hydrocarbon, the oxygen coverage on platinum would be high for the C_3H_8/O_2 system and low for the C_3H_6/O_2 one.

Solid Electrolyte Potentiometry (SEP) Measurements

SEP was proposed by Wagner (45) in order to probe the oxidation state of the catalyst-electrode under working condition. The equilibrium potential, V_{WR0} (potential difference between working and reference electrodes under open-circuit conditions), is related to the thermodynamic activity (a_o) of atomic oxygen adsorbed on platinum by

$$V_{WR0} = \frac{RT}{4F} \ln\left(\frac{a_o^2}{P_{O_2}^R}\right), \quad [6]$$

where R is the ideal gas constant, F the Faraday constant, T the absolute temperature, and $P_{O_2}^R$ the partial pressure of oxygen at the reference electrode, i.e., 0.21 atm. This equation is based on the existence of an equilibrium between O^{2-} in YSZ and oxygen adsorbed on the platinum surface [7], according to



Literature data are available dealing with the evolution of a_o with the temperature under reactive mixtures containing hydrocarbon, such as methane (46), butene (47), or propene (48). The lower temperature limit, for the use of solid electrolyte cells under equilibrium conditions with the Pt/YSZ system, has been determined to be around 250°C by comparing experimental values of V_{WR0} with those calculated by the Nernst equation. However, to deal with catalytic study

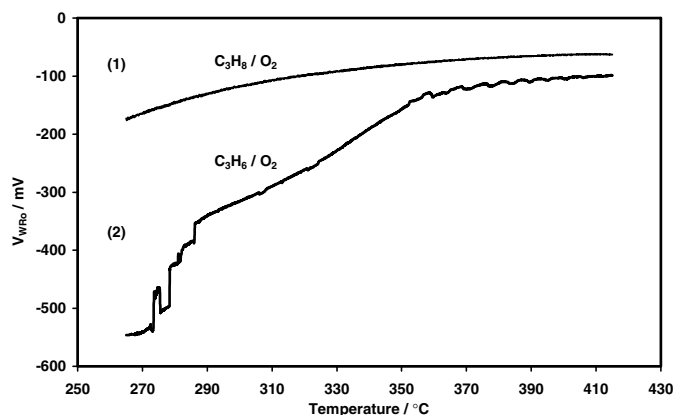


FIG. 5. Variation of the open-circuit voltage (V_{WR0}) versus temperature. The feed composition was (1) C_3H_8/O_2 : 2000 ppm/1% and (2) C_3H_6/O_2 : 2000 ppm/1%.

demands, Brück *et al.* (49) demonstrated that such measurements can be performed at temperatures somewhat lower than this limit, provided that stable values of V_{WR0} are obtained.

SEP measurements have been carried out under C_3H_8/O_2 and C_3H_6/O_2 as a function of the temperature. The corresponding variations of V_{WR0} , plotted in Fig. 5, show a gradual increase with an increase in temperature under C_3H_8/O_2 and an abrupt enhancement under C_3H_6/O_2 . This behavior can be correlated to what was observed for the catalytic activity (Fig. 3). This indicates that the oxygen activity on the catalyst surface directly connected to V_{WR0} is correlated to the hydrocarbon conversion. At low temperatures, below 290°C for propane and below 260°C for propene, V_{WR0} is stable with temperature and its value is -173 mV under propane and -546 mV under propene. This means that at low hydrocarbon conversion, the oxygen activity on the Pt surface is much lower under propene than under propane. At higher temperatures, above 400°C for propane and above 350°C for propene, V_{WR0} is close to -60 mV under C_3H_8/O_2 and -100 mV under C_3H_6/O_2 . The oxygen activity on Pt, probably linked to the oxygen coverage, is highest when hydrocarbon conversion is maximal. Kaloyannis and Vayenas (5) have reported V_{WR0} variation with the propene partial pressure at 430°C. Their study confirms our results since they found that when the propene partial pressure exceeds a value slightly lower than that corresponding to the stoichiometry, then propene coverage on Pt largely exceeds oxygen coverage.

Temperature-Programmed Desorption (TPD) Measurements

Peaks at $m/e = 29$ and 41, representative of propane and propene, respectively, were first recorded versus sample temperature in order to verify if unreacted propane or propene molecules are still present at Pt surface after the

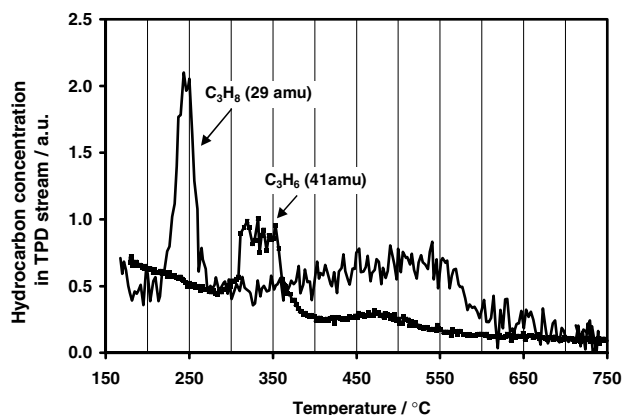


FIG. 6. Profiles corresponding to unreacted propane (at 29 amu) and propene (at 41 amu) molecules desorbing from the YSZ-supported Pt powder after propane or propene combustion, respectively.

catalytic reaction. The correction was made for the relative sensitivity factors of our mass spectrometer. The corresponding profiles (Fig. 6) indicate that small amounts of unreacted hydrocarbons desorb. The amount of unreacted hydrocarbon molecules detected during these desorption experiments is far lower than the quantity corresponding to one monolayer coverage of surface platinum. It is plausible that such a small quantity of unreactive propane and propene remains adsorbed on platinum at quite a low temperature. Differences in desorption temperatures (250°C for C_3H_8 and 330°C for C_3H_6) suggest that propene is more strongly adsorbed than propane. Broad structures at higher temperatures can be attributed to a nonspecific desorption process, probably from the reactor walls. More information can be drawn from a signal at 15 amu, corresponding to CH_3^+ ions resulting from fragmentation of hydrocarbons. The corresponding profiles are shown in Fig. 7. Intensities of the TPD peak at $m/e = 15$ amu are much

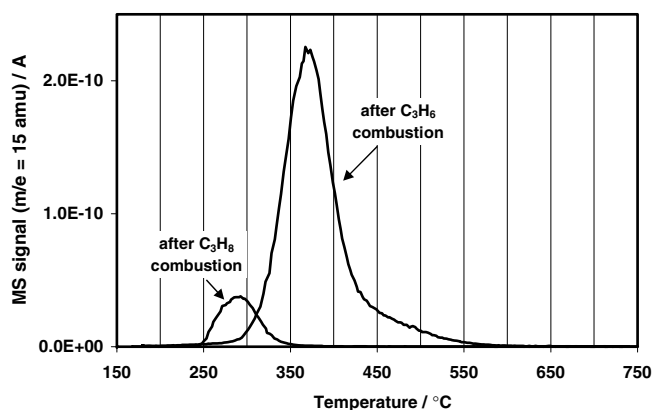


FIG. 7. Profiles corresponding to CH_3^+ ion detection (at 15 amu) during TPD of the YSZ-supported Pt powder after propane or propene combustion.

higher (more than one order of magnitude) than one could expect from the intensity of TPD peaks at $m/e = 29$ and 41 amu. This indicates that these peaks originate from the desorption of hydrocarbon fragments adsorbed on the catalyst (surely on precious metal particles). We observed no additional desorption of carbonaceous species ($C_2H_5^+$, for example) concomitant to the TPD peak at $m/e = 15$ amu. As propene and propane contain the same number of carbon atoms, we can directly compare the amplitude of signals plotted in Fig. 7. The catalyst submitted to propene combustion desorbs much larger amounts of CH_3^+ ions than the sample submitted to propane combustion; the ratio is ca. 100. In addition, the temperature of TPD peak maximum is 285°C for the catalyst submitted to propane combustion and 375°C for the catalyst submitted to propene combustion. These two observations clearly indicate that propene combustion at low conversion on Pt/YSZ leaves hydrocarbon fragments in larger amounts and which are more strongly bonded to the surface compared to the sample submitted to propane combustion. This is in full agreement with kinetic and SEP measurements obtained with these two hydrocarbons.

Catalytic Activity Measurements under Closed Circuit

At 344°C , after conversion stabilization at open-circuit voltage, a polarization V_{WR} was applied between the platinum working electrode and the gold reference electrode. Both electrodes were exposed to the same atmosphere, C_3H_8/O_2 or C_3H_6/O_2 . The reactive mixture had the same composition as for previous SEP and TPD measurements, i.e., 2000 ppm of hydrocarbon and 1% of oxygen. The profiles plotted in Fig. 8 allow comparison of the evolution of ρHC (rate enhancement of the catalytic reaction) versus time in C_3H_8/O_2 and C_3H_6/O_2 . At time zero, $V_{\text{WR}} = +3$ V was applied under propane and $V_{\text{WR}} = -3$ V under propene.

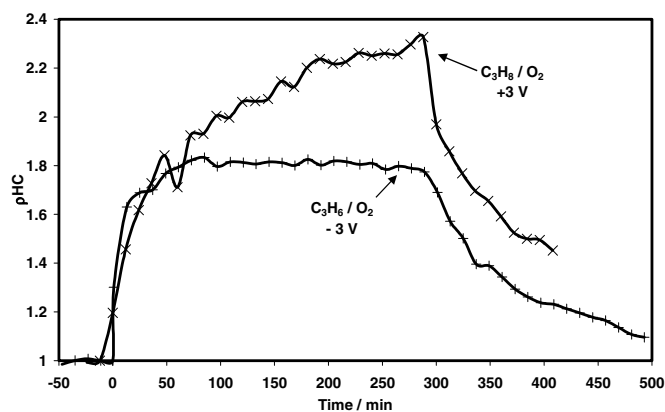


FIG. 8. Variation of the rate enhancement ratio (ρHC) versus time at $T = 344^\circ\text{C}$ under C_3H_8/O_2 : 2000 ppm/1% and upon an applied voltage $V_{\text{WR}} = +3$ V (\times), and under C_3H_6/O_2 : 2000 ppm/1% and upon an applied voltage $V_{\text{WR}} = -3$ V ($+$).

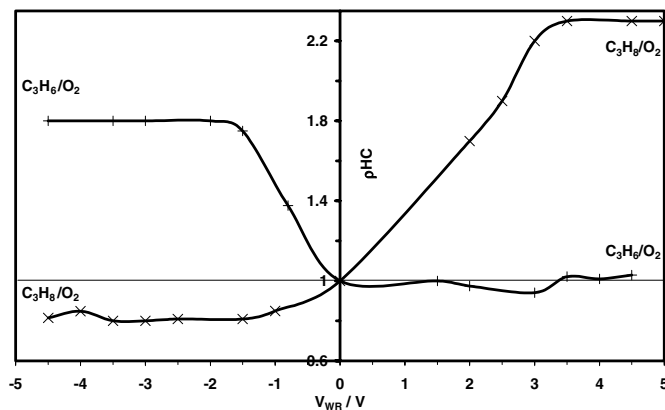


FIG. 9. Variation of the rate enhancement ratio (ρHC) versus V_{WR} at $T = 344^\circ\text{C}$ under C_3H_8/O_2 : 2000 ppm/1% (\times) and under C_3H_6/O_2 : 2000 ppm/1% ($+$).

It must be noted that the voltage reported here includes the ohmic drop, which mainly corresponds to the YSZ resistivity. In both cases, the rate of hydrocarbon oxidation increases upon an applied overvoltage. This means that the potential effect is opposite, according to the nature of hydrocarbon. Propane oxidation exhibits electrophobic enhancement while propene oxidation is electrophilic. The variations of ρ with time are also very different. In C_3H_8/O_2 , the promoting effect is gradual whereas in C_3H_6/O_2 it is abrupt. We observed previously the same trend during both catalytic activities from OCV and SEP measurements. In C_3H_8/O_2 atmosphere, hydrocarbon conversion increases from 4.3 to 10.1% upon application of +3 V, whereas under C_3H_6/O_2 , it enhances from 17.8 to 31.8% upon application of -3 V. The current at the Pt/YSZ interface slightly increases with time in C_3H_8/O_2 , from 33 to $40 \mu\text{A}$, whereas in C_3H_6/O_2 it decreases from -60 to $-78 \mu\text{A}$. The faradaic efficiency Λ reaches +123 in C_3H_8/O_2 and -60 in C_3H_6/O_2 . After 280 min of polarization, the applied voltage was turned off and catalytic activity gradually decreased. Figure 9 shows the evolution of ρHC versus V_{WR} at 344°C . The enhancement ratio ρHC corresponds to the steady state, i.e., after more than 4 h of polarization in the case of propane oxidation and after only 1 h in the case of propene oxidation. A positive potential enhances the propane oxidation and has no effect on the propene oxidation. An important fact is that a negative potential has a promoting effect on propene conversion and an inhibiting effect on propane oxidation. In C_3H_8/O_2 , a low negative potential, -1 V, which corresponds to very low current (lower than $10 \mu\text{A}$), is sufficient to reach minimal value of ρHC , while $+3.5$ V is necessary to obtain a maximal enhancement. The inhibiting effect of potential or current on the propane conversion becomes more pronounced when the reactive mixture contains larger amounts of oxygen. For instance, in C_3H_8/O_2 : 7120 ppm/8.9% O_2 , the composition

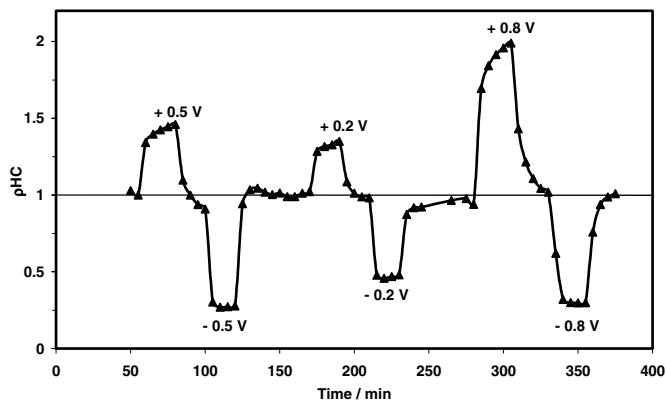


FIG. 10. Variation of the rate enhancement ratio (ρ_{HC}) versus time at $T = 365^\circ\text{C}$ under $\text{C}_3\text{H}_8/\text{O}_2$: 7120 ppm/8.9% and upon applied voltages $V_{WR} = +0.5, -0.5, +0.2, -0.2, +0.8,$ and -0.8 V.

used during the catalytic activity measurements at OCV, the catalytic rate can be reduced by a factor of 3 at 365°C (Fig. 10). The propane conversion varies from 7% upon application of -0.8 V to 47% upon application of $+0.8$ V. At very low potential, ± 0.2 V, the inhibiting effect is much more effective than the promoting one. The faradaic efficiency is $+1650$ for $+0.2$ V and $+14,260$ for -0.2 V. Upon application of $+0.8$ V, Λ is $+36$ while it is $+1930$ upon application of -0.8 V.

DISCUSSION

The present work shows that the NEMCA effect, in complete oxidation on Pt/YSZ, can be markedly different according to the nature of the hydrocarbon. Propane and propene were selected, because of their identical carbon content and their similar size. The oxidation of these hydrocarbons depends on their competitive adsorption with oxygen on platinum surface and consequently depends on the platinum oxygen coverage, θ_{O} . This last parameter varies with gas-phase oxygen content and with temperature.

Catalytic activity at OCV, SEP, and TPD measurements clearly show the following.

- Under oxygen-rich conditions, propene oxidation starts about 50°C below that of propane oxidation. The propane oxidation rate gradually increases whereas that of the propene abruptly rises with temperature.

- The oxygen thermodynamic activity (a_{O}) on the catalyst surface is lower under propene than under propane. It follows the changes in hydrocarbon conversion according to the temperature.

- Propene is much more strongly adsorbed on Pt than is propane. Propene combustion, at low conversion, leaves hydrocarbon fragments in larger amounts and which are more strongly bonded to the surface compared to the catalyst submitted to propane combustion.

The following can be suggested:

- Under $\text{C}_3\text{H}_8/\text{O}_2$ atmosphere, oxygen is more strongly adsorbed than propane on platinum, i.e., at low propane conversions, the oxygen coverage is high.
- Under $\text{C}_3\text{H}_6/\text{O}_2$ atmosphere, propene is more strongly adsorbed than oxygen on platinum. Then, at low propene conversions, θ_{O} is low. When the oxidation is complete, θ_{O} increases and platinum surface is mainly covered by oxygen until 450°C , a temperature at which oxygen desorption starts.

Propane and propene oxidation show opposite behaviors upon applied overpotentials:

- The propane oxidation exhibits electrophobic behavior with enhancement of its catalytic activity upon positive applied overpotentials. We also observed a decreasing of the propane oxidation rate upon application of negative voltages. An important point is that this reaction rate can be significantly controlled via voltage application. For instance, at 365°C , the polarization of platinum deposited on YSZ allows obtainment of a wide domain of C_3H_8 conversion, from 7 to 47%.

- The propene oxidation exhibits electrophilic properties; i.e., a negative current or potential can enhance its rate within a temperature range from lights off to complete oxidation. Note that this temperature range is narrow because of its abruptly rising oxidation rate. Kaloyannis and Vayenas (5) reported the same behavior concerning propene oxidation upon applied overvoltages.

Previous studies have shown that the catalytic oxidation of CH_4 (4) and C_2H_6 (6), on the Pt/YSZ system, is strongly promoted by positive overvoltages. These manifestations of electrochemical promotion have been related to the spillover of oxide ions (O^{2-}) from YSZ to the platinum surface. The consequence is a greater mobility of adsorbed oxygen, and then a decreasing of oxygen coverage which favors the hydrocarbon adsorption. This assumption was confirmed in a previous study, using cyclic voltammetry and impedance spectroscopy, of propane oxidation on Pt/YSZ (50). Such preliminary observations may help us to explain the behavior differences between propane and propene according to electrochemical promotion of total oxidation reaction.

According to the classification of Vayenas (38), propane is considered an electron-donor and oxygen an electron acceptor. Our SEP and TPD experiments have shown that this hydrocarbon is weakly bonded to the platinum surface and that oxygen coverage is high, under open-circuit conditions. Applying a positive polarization ($V_{WR} > 0$) produces migration (by electrochemical pumping) of O^{2-} species, strongly bonded to the surface platinum. Such species are not expected to take a direct part in the oxidation reaction but the result of their presence is that oxygen species coming from the gas phase are more weakly bonded.

Moreover, applying a positive potential strengthens the bond of electron-donor adsorbates (propane) and weakens the bond of electron-acceptor adsorbates (oxygen). These three effects converge to enhance the reactivity of oxygen present on the surface and then the rate of propane oxidation reaction when positive potential is applied. The consequence of a truly electrophobic behavior, according to the original definition, should be a partial inhibition of the corresponding reaction when a negative overpotential is applied. The system investigated here exhibits such a behavior, which is scarcely reported in the literature but was observed, for example, in the case of ethylene oxidation (51). The consequence of applying a negative overpotential is, according to Ref. (38), to weaken Pt–hydrocarbon bonds and to strengthen Pt–oxygen bonds. The result is to lower the hydrocarbon coverage (which was already very low) and to make oxygen less reactive. These two effects should converge to lower the oxidation reaction rate. Moreover, electrochemically pumped O^{2-} flow is directed from the platinum toward the YSZ, and then only a detrimental effect can be expected.

Concerning propene, this hydrocarbon is also classified by Vayenas as an electron donor, as is predictable from the presence of π -electrons in its structure. The first step of adsorption may be the formation of a π -complex between Pt and propene. Applying a positive potential brings O^{2-} species onto the platinum surface. The effect should be to enhance the reactivity of surface oxygen species coming from the gas phase, but such species are few because propene is predominantly and strongly adsorbed on platinum at OCV. In addition, the bond between the hydrocarbon and platinum becomes stronger. Therefore, no beneficial effect can be expected, in agreement with our experimental observations. When a negative overpotential is applied, Pt–propene bonds are made weaker, because of the increase of electron density on platinum. This phenomenon is expected from all electron donors, but the corresponding effect must be particularly drastic in the case of propene, according to its adsorption mode involving π -electrons. The second consequence of a negative overpotential is to make Pt–O bonds stronger. These two effects may justify the enhancement of the oxidation reaction by increasing the θ_O/θ_{HC} ratio.

It is noteworthy that the kinetics of the rate enhancement of the propane oxidation upon application of +3 V is much lower than that of propene upon application of –3 V. Disregarding the fact that propene is easier to oxidize than propane, this could indicate that the rate of O^{2-} spillover between YSZ and Pt, in the case of propane oxidation, induces a gradual promotional effect. In contrast, the effect of negative overpotentials on the propene oxidation is fast and stabilizes after only few minutes. This could suggest that electrochemical promotion upon negative overpotentials is mainly due to the electric field effect and not to the backspillover of oxide ions.

CONCLUSIONS

The full oxidation of both propane and propene on Pt/YSZ can be electrochemically promoted. This promotion exhibits a NEMCA effect, with the reaction rate increasing much more than is predicted from the Faraday law. The hydrocarbon oxidation rates can be significantly controlled via voltage application, in a reversible manner. The two hydrocarbons exhibit opposite behaviors upon applied overpotentials. Full oxidation of propane is enhanced when a positive overpotential is applied to the catalyst-electrode and, conversely, the oxidation rate of propene is increased under a negative polarization. These differences are attributed to competitive adsorption between oxygen and the hydrocarbons. In C_3H_8/O_2 atmosphere, under open-circuit conditions, oxygen coverage (θ_O) on Pt is high and an electrophobic NEMCA effect is observed, as reported in the literature with other alkanes. In C_3H_6/O_2 atmosphere, propene is predominantly and strongly adsorbed on Pt, and then a negative potential enhances propene oxidation rate by increasing θ_O , according to an electrophilic NEMCA effect. The NEMCA behavior of a catalytic reaction which occurs on a catalyst deposited on an electrolyte conductor by oxygen ions is dependent on the oxygen coverage at OCV. These results prove that the application of a current or a potential through the Pt/YSZ system does modify both the hydrocarbon and the oxygen coverages on the catalyst. This is in agreement with the need to consider the rate dependence on the electron-donor and electron-acceptor partial pressures, as stated by Vayenas *et al.* in a recent paper on the rules of electrochemical promotion (38).

ACKNOWLEDGMENTS

The authors gratefully acknowledge the financial support of the PREDIT programme (ADEME) and ECODEV (CNRS).

REFERENCES

1. Vayenas, C. G., Bebelis, S., and Ladas, S., *Nature (London)* **343**, 625 (1990).
2. Vayenas, C. G., Bebelis, S., Yentekakis, I. V., and Lintz, H. G., *Catal. Today* **11**, 303 (1992).
3. Vayenas, C. G., Jaksic, M. M., Bebelis, S., and Neophitides, S. G., in "Modern Aspects of Electrochemistry" (J. O. M. Bockris, B. E. Conway, and R. E. White, Eds.), Vol. 29, p. 57. Plenum, New York, 1996.
4. Tsiakaras, P., and Vayenas, C. G., *J. Catal.* **140**, 53 (1993).
5. Kaloyannis, A., and Vayenas, C. G., *J. Catal.* **182**, 37 (1999).
6. Kaloyannis, A., and Vayenas, C. G., *J. Catal.* **171**, 148 (1997).
7. Petrolekas, P. D., Balomenou, S., and Vayenas, C. G., *J. Electrochem. Soc.* **145** (4), 1202 (1998).
8. Vayenas, C. G., Bebelis, S., and Despotopoulou, M., *J. Catal.* **128**, 415 (1991).
9. Yentekakis, I. V., Palermo, A., Filkin, N. C., Tikhov, M. S., and Lambert, R. M., *J. Phys. Chem. B* **101**, 3759 (1997).
10. Petrolekas, P. D., Brosda, S., and Vayenas, C. G., *J. Electrochem. Soc.* **145** (5), 1469 (1998).

11. Makri, M., Buekenhoudt, A., Luyten, J., and Vayenas, C. G., *Ionics* **2**, 282 (1996).
12. Balomenou, S., Pitselis, G., Polydoros, D., Giannikos, A., Vradis, A., Frenzel, A., Pliangos, C., Pütter, H., and Vayenas, C. G., *Solid State Ionics* **136–137**, 857 (2000).
13. Tsiplakides, D., Neophytides, S., Enea, O., Jaksic, M. M., and Vayenas, C. G., *J. Electrochem. Soc.* **144**(6), 2072 (1997).
14. Yentekakis, I. V., and Vayenas, C. G., *J. Catal.* **149**, 238 (1994).
15. Pliangos, C., Yentekakis, I. V., Ladas, S., and Vayenas, C. G., *J. Catal.* **159**, 189 (1996).
16. Ladas, S., Kennou, S., Bebelis, S., and Vayenas, C. G., *J. Phys. Chem.* **97**, 8845 (1993).
17. Palermo, A., Tikhov, M. S., Filkin, N. C., Lambert, R. M., Yentekakis, I. V., and Vayenas, C. G., *Stud. Surf. Sci. Catal.* **101**, 513 (1996).
18. Jiang, Y., Yentekakis, I. V., and Vayenas, C. G., *J. Catal.* **148**, 240 (1994).
19. Neophytides, S. G., and Vayenas, C. G., *J. Phys. Chem.* **99**, 17063 (1995).
20. Neophytides, S. G., Tsiplakides, D., and Vayenas, C. G., *J. Catal.* **178**, 414 (1998).
21. Tsiplakides, D., Neophytides, S., and Vayenas, C. G., *Solid State Ionics* **136–137**, 839 (2000).
22. Vayenas, C. G., Ionnides, A., and Bebelis, S., *J. Catal.* **129**, 67 (1991).
23. Makri, M., Vayenas, C. G., Bebelis, S., Besocke, K. H., and Cavalca, C., *Surf. Sci.* **369**, 351 (1996).
24. Frantzis, A. D., Bebelis, S., and Vayenas, C. G., *Solid State Ionics* **136–137**, 863 (2000).
25. Nicole, J., Tsiplakides, D., Wodiunig, S., and Comminellis, C., *J. Electrochem. Soc.* **144**, 1312 (1997).
26. Tsiplakides, D., and Vayenas, C. G., *J. Electrochem. Soc.* **148** (5), E189 (2001).
27. Zipprich, W., Wiemhöfer, H.-D., Vohrer, U., and Göpel, W., *Ber. Bunsen-Ges. Phys. Chem.* **99**, 1406 (1995).
28. Williams, F. J., and Aldao, C. M., *Surf. Sci.* **425**, L387 (1999).
29. Vayenas, C. G., and Tsiplakides, D., *Surf. Sci.* **467**, 23 (2000).
30. Parsons, R., *J. Electroanal. Chem.* **422**, 202 (1997).
31. Vayenas, C. G., *J. Electroanal. Chem.* **486**, 85 (2000).
32. Metcalfe, I. S., *J. Catal.* **199**, 247 (2001).
33. Metcalfe, I. S., *J. Catal.* **199**, 259 (2001).
34. Vayenas, C. G., Bebelis, S., Yentekakis, I. V., and Lintz, H.-G., *Catal. Today* **11**, 303 (1992).
35. Bebelis, S., and Vayenas, C. G., *J. Catal.* **118**, 147 (1989).
36. Marwood, M., and Vayenas, C. G., *J. Catal.* **168**, 538 (1997).
37. Marwood, M., and Vayenas, C. G., *J. Catal.* **178**, 429 (1998).
38. Vayenas, C. G., Brosda, S., and Pliangos, C., *J. Catal.* **203**, 329 (2001).
39. Bebelis, S., Makri, M., Buekenhoudt, A., Luyten, J., Brosda, S., Petrolekas, P., Pliangos, C., and Vayenas, C. G., *Solid State Ionics* **139**, 33 (2000).
40. Burch, R., Crittle, D. J., and Hayes, M. J., *Catal. Today* **47**, 229 (1999).
41. Burch, R., and Watling, T. C., *Catal. Today* **43**, 19 (1997).
42. Konsolakis, M., Macleod, N., Isaac, J., Yentekakis, I. V., and Lambert, R. M., *J. Catal.* **193**, 330 (2000).
43. Anderson, A. B., Lang, D. B., and Kim, Y. J., *J. Am. Chem. Soc.* **106**, 6597 (1984).
44. Weaver, J. F., Krzyzowski, M. A., and Madix, R. J., *J. Chem. Phys.* **112** (1), 396 (2000).
45. Wagner, C., *Adv. Catal.* **21**, 323 (1970).
46. Eng, D., and Stoukides, M., *J. Catal.* **130**, 306 (1991).
47. Breckner, E. M., Sundaresan, S., and Benzinger, J., *Appl. Catal.* **30**, 277 (1987).
48. Hildenbrand, H. H., and Lintz, H. G., *Appl. Catal.* **65**, 241 (1990).
49. Brück, J., Lintz, H. G., and Valentin, G., *Solid State Ionics* **112**, 75 (1998).
50. Bultel, L., Hénault, M., Roux, C., Siebert, E., Béguin, B., Gaillard, F., Primet, M., and Vernoux, P., *Ionics* **136** (2002).
51. Wodiunig, S., Bokeloh, F., and Comminellis, Ch., *Electrochim. Acta* **46**, 357 (2000).